J. Anat. (2006) **209**, pp547–559 doi: 10.1111/j.1469-7580.2006.00641.x

Location of injury influences the mechanisms of both regeneration and repair within the MRL/MpJ mouse

Alice H. M. Beare, Anthony D. Metcalfe and Mark W. J. Ferguson

UK Centre for Tissue Engineering, Faculty of Life Sciences, University of Manchester, Manchester, UK

Abstract

The adult MRL/MpJ mouse regenerates all differentiated structures after through-and-through ear punch wounding in a scar-free process. We investigated whether this regenerative capacity was also shown by skin wounds. Dorsal skin wounds were created, harvested and archived from the same animals (MRL/MpJ and C57BL/6 mice) that received through-and-through ear punch wounds. Re-epithelialization was complete in dorsal wounds in both strains by day 5 and extensive granulation tissue was present by day 14 post-wounding. By day 21, wounds from both strains contained dense amounts of collagen that healed with a scar. The average wound area, as well as α-smooth muscle actin expression and macrophage influx were investigated during dorsal skin wound healing and did not significantly differ between strains. Thus, MRL/MpJ mice regenerate ear wounds in a scar-free manner, but heal dorsal skin wounds by simple repair with scar formation. A significant conclusion can be drawn from these data; mechanisms of regeneration and repair can occur within the same animal, potentially utilizing similar molecules and signalling pathways that subtly diverge dependent upon the microenvironment of the injury.

Key words blastema; regeneration; repair; scar; wound healing.

Introduction

Healing of an acute wound involves a reduction in wound size secondary to contraction and re-epithelialization and is accompanied by an increase in collagen deposition (Ashcroft et al. 1995, 1999). However, certain mammalian tissues are capable of spontaneous regeneration following injury (reviewed in Yannas, 2001). Skin wounds on early mammalian embryos heal perfectly with no signs of scarring and complete restitution of the normal skin architecture, whereas wounds to adult mammals often results in fibrosis and scar contracture with poor regeneration of epidermal and dermal structures at the site of the healed wound (Whitby & Ferguson, 1991a,b; see review by Ferguson & O'Kane, 2004).

One of the ultimate goals of biomedical science and tissue engineering is therapeutically to initiate controllable regeneration in adults, utilizing the mechanisms perfected by the embryo and other species. To achieve this, one of the challenges is to understand the basic tissue biology and the cellular and molecular mechanisms responsible for tissue repair and regeneration. Although numerous examples of complete regeneration exist in invertebrates, higher vertebrates such as amphibians demonstrate extensive but restricted regeneration, whereas mammals are severely limited in regenerative capacity.

To date, few examples of true adult mammalian regeneration have been described, and for this to be understood and harnessed as a tissue engineering therapy, a good model system needs to be identified. The rabbit ear model extensively studied by Goss & Grimes (1975) demonstrated a departure from the normal mammalian dermal repair process, with extended epithelial proliferation and migration, as well as dermal growth and the replacement of cartilage. More recently, Clark et al. (1998) described similar ear punch regeneration in the inbred MRL/MpJ mouse strain. In this model, 2-mm excisional wounds in the ears of the MRL/MpJ mouse were found to regenerate completely after 4–5 weeks, whereas in the control strain, C57BL/6, the excision remained almost intact. Our own studies

Correspondence
Professor Mark W. J. Ferguson, UK Centre for Tissue Engineering, Faculty of Life Sciences, University of Manchester, Manchester, UK.
T: +44 (0)161 2756775; F: +44 (0)161 2755945;
E: mark.w.ferguson@manchester.ac.uk

The first two authors contributed equally to this paper.

Accepted for publication *26 August 2006*

have shown, however, that C57BL/6 mice have the ability partially to regenerate through-and-through holes made to their ears (Rajnoch et al. 2003; Metcalfe & Ferguson, 2005). Attempts to understand the genetics thought to be responsible for this phenomenon had been studied, and genomic-level quantitative trait loci (QTL) mapping has been performed (McBrearty et al. 1998). This method demonstrated that candidate genes for ear regeneration were present on most of the mouse chromosomes and could not elucidate any single gene or combination of genes responsible for regeneration. Interestingly some studies suggest that loci-to-loci interactions may play a major role in tissue regeneration in the MRL/MpJ mouse (Masinde et al. 2001; Yu et al. 2005). Other studies have suggested that components of the inflammatory system may play a significant role in the regeneration/repair process (X. Li et al. 2000, 2001; F. Li et al. 2001; Gawronska-Kozak, 2004; Ueno et al. 2005; Gawronska-Kozak et al. 2006). Recently, restrictive fragment differential display-PCR has been used in an attempt to identify the genes involved in scar-free wound healing (Masinde et al. 2005). This study identified over 30 genes differentially expressed in the MRL/MpJ mice or C57BL/6 mice, which include some known to have a role in wound healing and others that do not (Masinde et al. 2005).

We have previously described that the MRL/MpJ regenerating ear model demonstrates considerable variability (Rajnoch et al. 2003). The extent of complete regeneration was dependent on the degree of trauma imposed, with wounds created by a blunt ear punch much less likely to regenerate than those created by a sharp surgical biopsy punch. This suggests that the regenerative capacity of the MRL/MpJ mouse may only occur under specific conditions, and when minimal necrosis occurs. It was also determined that the C57BL/6 control mouse possessed a limited regenerative capacity, with biopsy punch wounds closing to approximately half their original size by the end of the time course. This was in contrast to the original phenotype description of these mice after ear wounding, where a less significant decrease in wound size was observed.

In this study we demonstrate further variability in the MRL/MpJ regenerative response. We have already shown that MRL/MpJ mice can completely regenerate 2-mm through-and-through ear punch wounds without scarring (Rajnoch et al. 2003). This raised the question as to whether wounding the animal in another location led to the same regenerative healing. Consequently, at the same time that the ears were wounded, 4-mm punch biopsy excisional wounds were also created in the backs of the same animals, and these were harvested and analysed. We have found that MRL/MpJ mice that display accelerated healing and regeneration within their ears simply repair their back wounds with scarring. These results confirm and expand upon a recent study by Colwell et al. (2006). In our present study, in the dorsal skin wounds, scars of similar size and quality to those of the control animals were observed. A number of markers of wound repair, inflammation and scar formation were examined in the dorsal skin wounds and minimal differences were found between the two strains of mice. The mechanistic differences influencing regeneration and repair observed in the MRL/MpJ animals are as yet unknown.

Materials and methods

Animals

A breeding colony of MRL/MpJ mice, originally obtained from Jackson Laboratories, Bar Harbor, ME, USA, was established at the University of Manchester Biological Sciences Unit. Male and female mice of 8–10 weeks of age were used in all wounding experiments. C57BL/6 mice were obtained from Harlan UK Ltd (Bicester, UK). All procedures were carried out according to UK Home Office regulations and under appropriate licences.

Wounding

A standardized wounding template was used in both the ear and the back. A 2-mm-diameter through-and-through hole was punched in the centre of each ear using a clinical biopsy punch; these wounds were analysed previously (Rajnoch et al. 2003). At the same time, and on the same animals, two 4-mm punch biopsy excisions were created on the dorsum by pinching the skin at the midline and punching through both layers at the same time on to a cork board. All wounds were left untreated until the animal was killed by CO_2 exposure and cervical dislocation at the time points outlined below.

The complete time course and numbers for each time point were as follows: 3 days ($n = 3$), 5 days ($n = 3$), 7 days ($n = 3$), 14 days ($n = 3$), 21 days ($n = 3$), 28 days ($n = 3$), 35 days ($n = 3$), 56 days ($n = 4$), 84 days ($n = 4$).

Histology

The regenerative capacity of MRL/MpJ ear wounds was described previously (Rajnoch et al. 2003). Wounds from the backs of the same animals were excised with 2–3 mm of surrounding tissue, and either frozen in a liquid nitrogen vapour phase before being placed in OCT for cryosectioning or alternatively fixed in 10% neutral buffered formalin and processed for paraffin wax histology as previously described (Rajnoch et al. 2003). The entire block was sectioned and sections retained in two different ways. For dorsal wound map profiles, a single slide containing four adjacent sections was retained every 50 μm to create an evenly spaced collection. For immunohistochemical analysis, groups of ten slides, again with four adjacent sections per slide, were retained every 200 μm to create a grouped collection of adjacent and therefore directly comparable sections. Approximately 3–4 groups were collected per dorsal wound. One wound from each animal was sectioned in each of the above ways. For wound profile analysis, sections were stained with Masson's trichrome. Briefly, sections were dewaxed and rehydrated through graded alcohols, then stained with Harris' haematoxylin for 4 min, blued in tap water for 5 min, then stained with 1% picric acid in 70% ethanol for 30 s. After a brief rinse, sections were stained in 1% Biebrich Scarlet for 1 min followed by a very brief rinse, then for 10 min in PMA/PTA. Finally, the sections were stained in Fast Green for 5 min, rinsed, dehydrated and mounted.

Wound profiling and analysis

Under bright-field microscopy, digital images of one section from each slide of the wound were collected. All images from a single wound were taken at the same magnification. For analysis, Image ProPlus software was used to measure a number of parameters of the wound. The total linear wound width of each section was recorded, as was the wound contour, which follows the predicted path of the migrating epithelia, and in later stage wounds follows the completed epithelial layer from one margin of the wound to the other. At time points where scars were present, the extent of the granulation tissue margins was also measured.

All measurements were converted to a pixel equivalent and plotted onto graph paper so that a collated map was created for each wound. By this method the shape of the wound could be determined, and the total wound area could also be calculated, using the following equation:

$$\text{area} = \sum \text{WC}_{1-n} * 7 \times 10^{-5}$$

where WC is the wound contour measurement and 7×10^{-5} is the conversion from micrometres to millimetres and allows for the distance between each section.

Immunohistochemistry

Sections were stained using peroxidase immunohistochemical techniques to markers of cell proliferation, myofibroblast differentiation, inflammatory cells and apoptosis. The following general protocol was used. Wax sections were dewaxed and rehydrated as above. Sections were blocked against endogenous peroxidase using hydrogen peroxide in methanol, rinsed and then blocked using normal serum from the secondary antibody host. Primary antibodies [Mac-3, BD Pharmingen (550292), 1.5 μg mL^{-1} and α-SMA, Sigma Aldrich (A2547), 5.5 μg mL^{-1}] were diluted in blocking serum and applied to the sections and incubated overnight at 4 °C. The following day sections were rinsed and incubated with biotinylated secondary antibody also diluted in blocking serum. Vectastain ABC kit was applied to rinsed sections, then detection was performed using DAB substrate. Finally, sections were counterstained using nuclear fast red, dehydrated and mounted.

Results

In an earlier study we have demonstrated that MRL/MpJ ear wounds completely and perfectly regenerate all the differentiated structures of the ear without scarring (Rajnoch et al. 2003). This was consistent with the original discovery reported by Clark et al. (1998). The aim of the present study was to determine if MRL/MpJ dorsal wounds healed in a similar way. We used back wounds that were created, harvested and archived from the same animals used in our original study (Rajnoch et al. 2003). All MRL/MpJ dorsal wounds analysed were thus taken from animals with proven regenerative capacity of the ear. Sample photographs from the dorsal wounding time course are shown in Figs 1–5. All figures show an image of the centre of the wound, and Figs 1–3 also show a wound edge image from the same block. All images are representative of the time point.

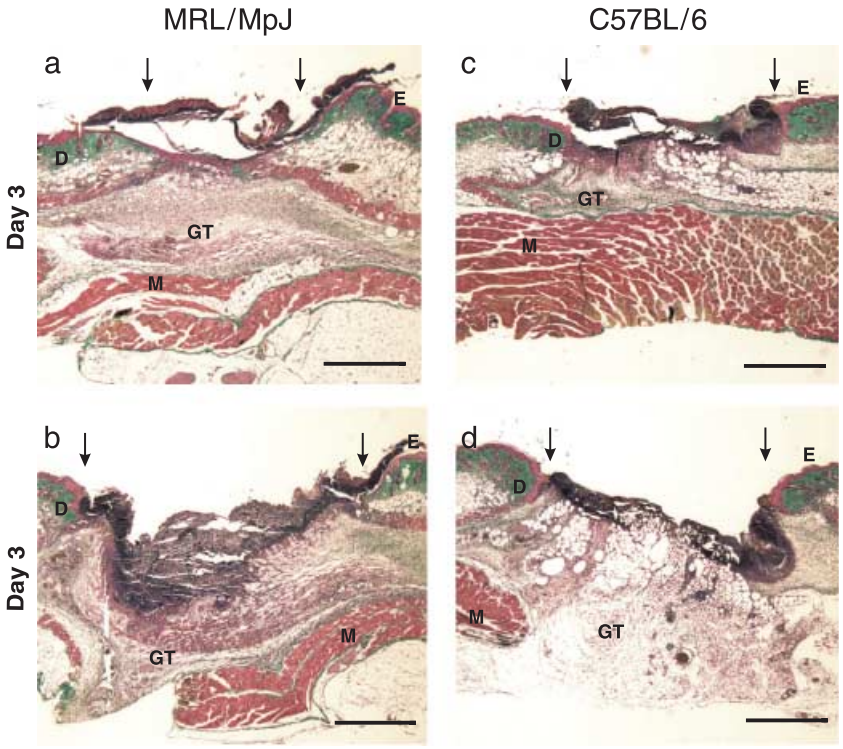

Fig. 1 Day 3 wound sections showing different regions of the wound: (a) MRL/MpJ wound margin, (b) MRL/MpJ wound centre, (c) C57BL/6 wound margin, (d) C57BL/6 wound centre. GT, granulation tissue; E, epithelium; D, dermis; M, muscle. Arrows denote wound margins. Scale bar = 1 mm.

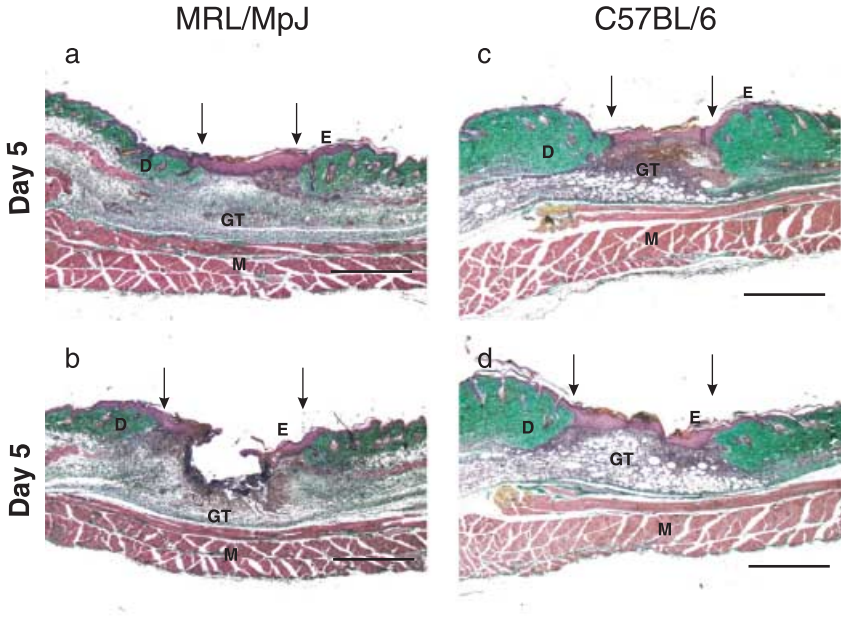

Fig. 2 Day 5 wound sections showing different regions of the wound: (a) MRL/MpJ wound margin, (b) MRL/MpJ wound centre, (c) C57BL/6 wound margin, (d) C57BL/6 wound centre. GT, granulation tissue; E, epithelium; D, dermis; M, muscle. Arrows denote wound margins. Scale bar = 1 mm.

The wound healing process proceeded normally in all wounds. By day 3 post-injury (Fig. 1) some provisional matrix was observed in the wound centre, but a clot was still present over the wound (Fig. 1b,d). Some re-epithelialization had begun, as shown in Fig. 1(a). At this stage there appeared to be slight differences in the amount of re-epithelialization between the two strains with the MRL/MpJ wounds demonstrating more epithelial migration than C57BL/6 at the margin.

By day 5 (Fig. 2) significant wound contraction had occurred and there was more granulation tissue at the wound margins and wound centre. The wound margins were covered with a thick epithelium and the early enhancement of re-epithelialization observed at day 3

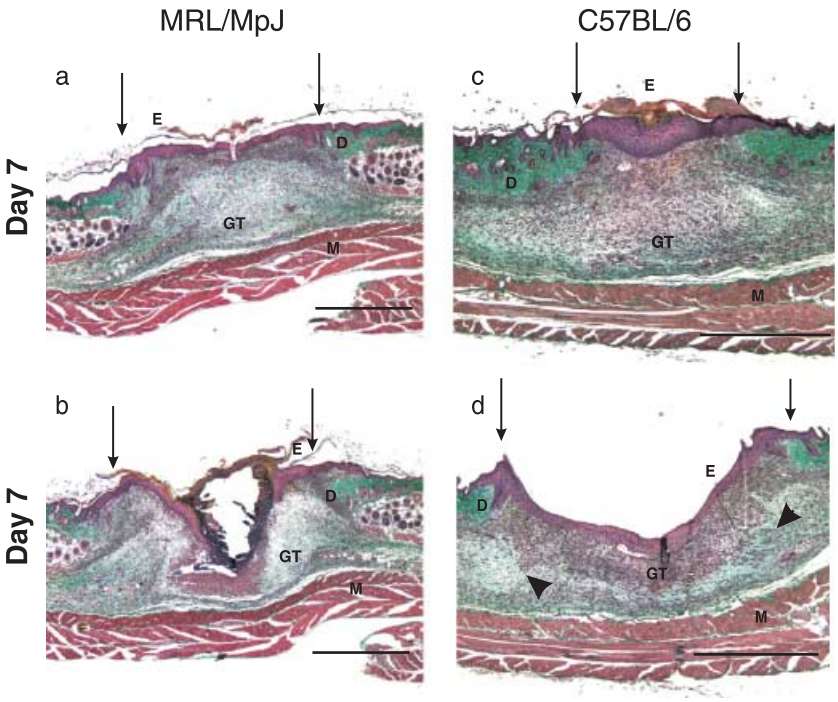

Fig. 3 Day 7 wound sections showing different regions of the wound: (a) MRL/MpJ wound margin, (b) MRL/MpJ wound centre, (c) C57BL/6 wound margin, (d) C57BL/6 wound centre – arrowheads denote areas of collagen deposition within the granulation tissue. GT, granulation tissue; E, epithelium; D, dermis; M, muscle. Arrows denote wound margins. Scale bar = 1 mm.

in the MRL/MpJ wounds had diminished. At this stage there was considerable epithelialization over the centre of the C57BL/6 wound (Fig. 2d).

At day 7 (Fig. 3) there was evidence of collagen deposition in the granulation tissue of all wounds, with matrix stained blue–green by the Masson's trichrome appearing at the edges of the wound area (Fig. 3d). Re-epithelialization was almost complete with a thick epithelium present across most of the wound section in both MRL/MpJ and C57BL/6 mice. Some variation in wound shape was observed; however, the repair process progressed in both strains.

By day 14 (Fig. 4a,b) the apparent variation between strains had disappeared, with all wounds well granulated and completely re-epithelialized. The granulation tissue was maturing, with increasing collagen deposition and a decrease in cellularity, probably due to apoptosis. The epithelial thickness decreased and the epithelium appeared mature. There was little visible difference between the wound epithelium and that of the normal skin. The wound was still visible due to an increase in tissue thickness compared with normal skin, but there was an absence of differentiated structures (hair follicles and sebaceous glands). In contrast to our earlier study in the wounded ear at this time point (Rajnoch et al. 2003), where blastema-like structures were readily identifiable; no such structures were observed in the healing back wounds. The earlier indicators of the wound site became less obvious from 21 days post-wounding onwards (Fig. 4c–f). The dermis became thinner and collagen deposition was more evenly distributed, matching more closely the surrounding tissue; this was observed to continue at day 35 post-wounding.

By day 56 (Fig. 5a,b) the scar was detectable integrated with the surrounding dermis, and the damaged panniculus carnosus muscle (arrowhead, Fig. 5b) had not regenerated. Apoptosis had progressed and there were few cells remaining within the dermis. By day 84 (Fig. 5c,d), the scar was still detectable and visible macroscopically by the uneven distribution of the hair follicles. This gap in follicle density is visible as the hair growth cycle proceeds but as the follicles regress into telogen the scar becomes less detectable microscopically.

Because the histological analysis revealed no major differences in the dorsal repair mechanisms between the two strains, an analysis of the wound areas was undertaken. Measurements of dorsal wound sections and calculation of wound areas showed that the MRL/MpJ dorsal wounds did not heal significantly faster than those of the C57BL/6 mice (Fig. 6). In fact, the wounds were usually slightly, but not significantly, larger ($P > 0.05$ in all cases, SPSS paired samples *t*-test)

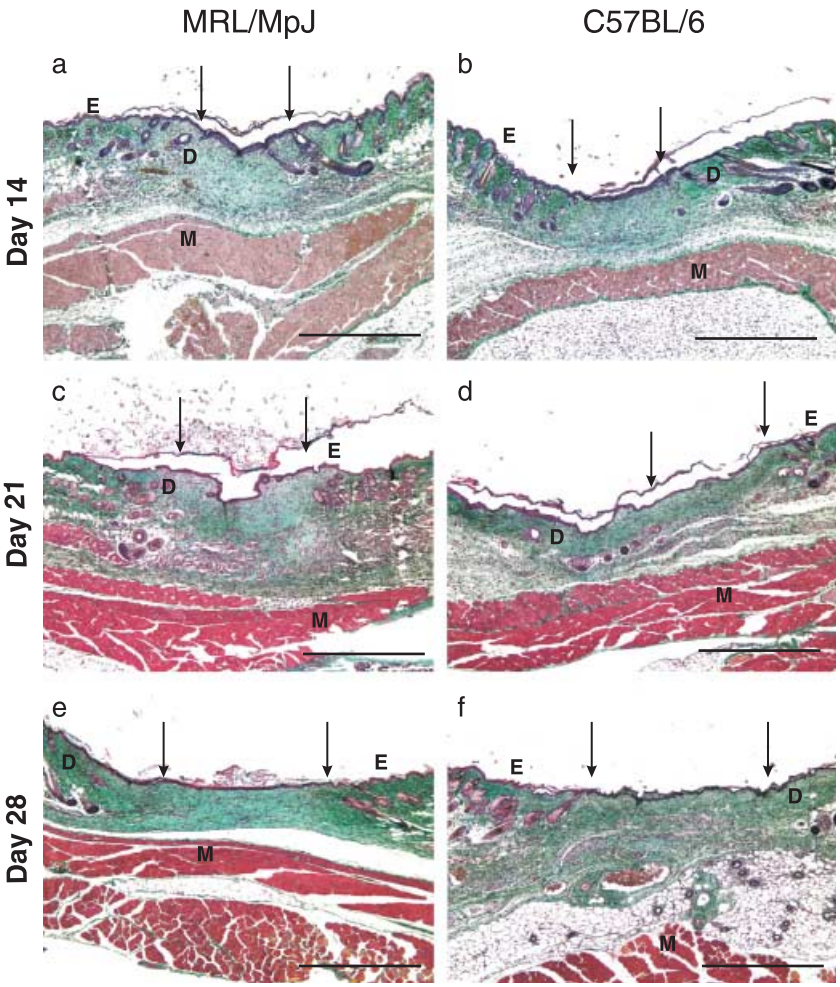

Fig. 4 Sections of the wound centres for the two strains at different time points. Day 14 (a – MRL/MpJ wound centre, b – C57BL/6 wound centre), day 21 (c – MRL/MpJ wound centre, d – C57BL/6 wound centre), day 28 (e – MRL/MpJ wound centre, f – C57BL/6 wound centre) wound sections. E, epithelium; D, dermis; M, muscle. Arrows denote wound margins. Scale bar = 0.5 mm.

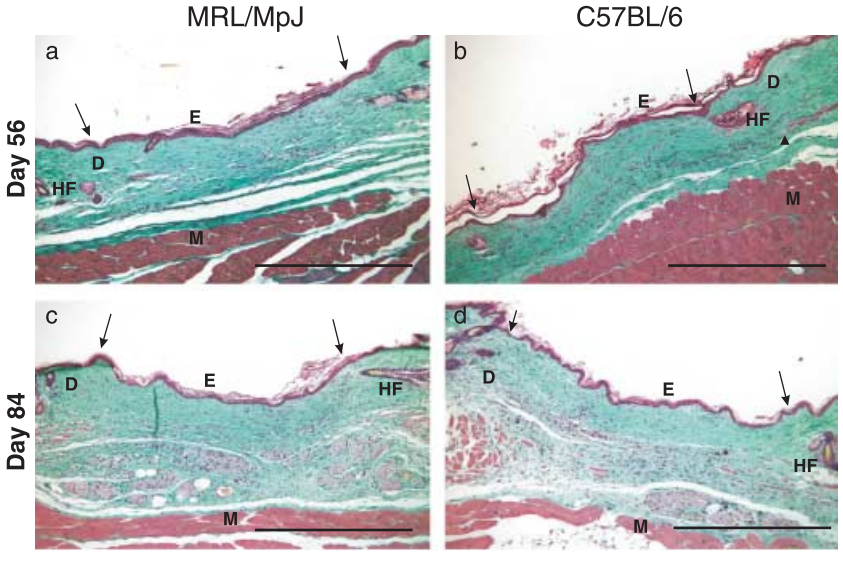

Fig. 5 Sections of the wound centres for the two strains at different time points. Day 56 (a – MRL/MpJ wound centre, b – C57BL/6 wound centre) and day 84 (c – MRL/MpJ wound centre, d – C57BL/6 wound centre) wound sections. HF, hair follicle; E, epithelium; D, dermis; M, muscle. Arrows denote wound margins. Scale bar = 0.5 mm.

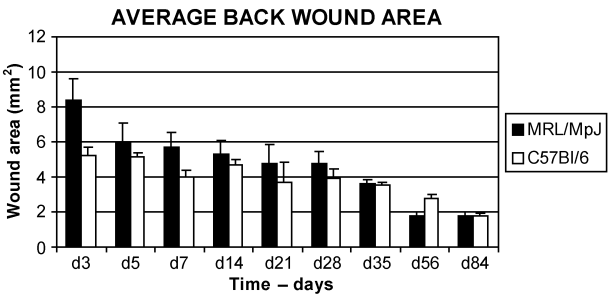

Fig. 6 Graph of collated wound surface areas. Total wound areas were calculated using data collected from the evenly spaced wound sections. Note that the MRL/MpJ wounds are slightly larger than the C57BL/6 wounds at the early time points, although not significantly so ($P > 0.05$). Also note that the day 84 wound areas are the same in both groups, indicative of similar sized scars, $n = 3$.

than the C57BL/6 wounds, despite the initial injury being the same size. By the end of the 84-day time course, both MRL/MpJ and C57BL/6 wounds were just less than 2 mm^2 in size (Fig. 6).

Additionally, and in contrast to the accelerated scar-less regeneration of the wounded ear tissue, the MRL/MpJ back wounds from the same animals healed with a scar. The size and quality of the MRL/MpJ back wound scars was the same as that of the C57BL/6 dorsal scars. In all cases the scar tissue was distinct from the surrounding normal tissue. Hair follicles and sebaceous glands were absent, and the scar matrix was arranged in a parallel, striated pattern as opposed to the basket weave pattern of normal dermis. These observations suggest that the mechanism responsible for regeneration in the MRL/MpJ ear is not functioning in the skin of the back of the same mice. The reason for this difference is currently unknown.

In order further to clarify the results of the histological analysis, markers of inflammation and dorsal wound contraction were examined using immunohistochemistry. An antibody specific for macrophages, Mac-3, demonstrated that the influx of macrophages into the wounds occurred similarly in both strains. Figure 7 shows sample images from the wound centre, margins and far edges of both strains of mice at day 3. Positive cell counts were made in the wound centre (Fig. 8a), at the wound margin (Fig. 8b) and in the dermis away from the wound (Fig. 8c) to compare the rate of macrophage influx into the wounds. There was no significant difference in the percentage of Mac-3-positive cells between the two mouse strains over the 7-day time course (Fig. 8). Although there was some variation in the profiles produced, the differences were not consistent or significant. The total cell counts obtained were very similar between the two groups (Fig. 8d), suggesting that any real difference was not obscured by variability in the cellularity of the wounds.

To determine further any subtle differences between the two strains with regard to dorsal wound contraction, sections were immunostained for alpha smooth

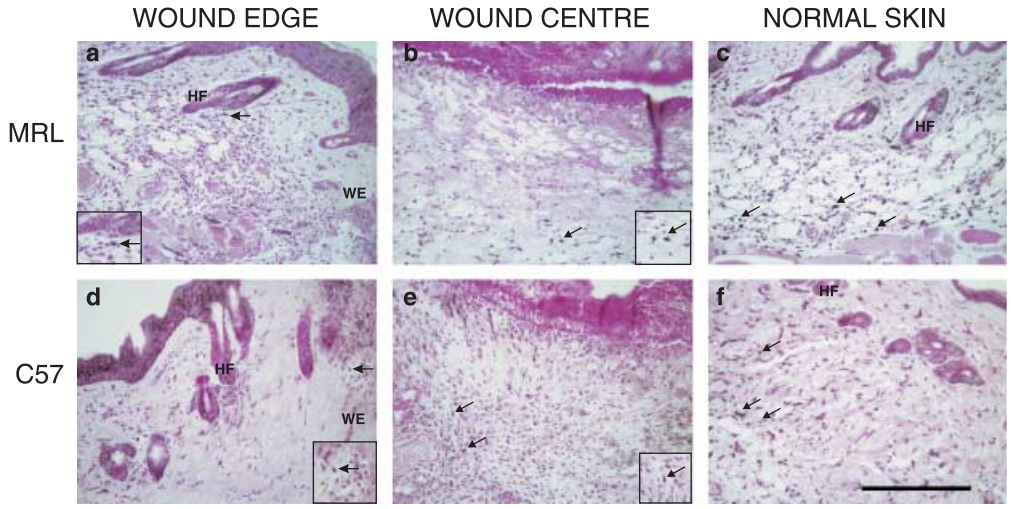

Fig. 7 Mac-3 staining for macrophages at the wound edge (a,d), wound centre (b,e) and in the normal skin to the side of the wound (c,f) in MRL/MpJ (a–c) and C57BL/6 (d–f) sections at 3 days post-injury. Note that there are few positive cells in the wound centre and margin at this time, but more in the normal skin away from the wound. WE = wound edge, HF = hair follicle, arrows denote positively stained cells. Insets (a,b,d,e) are a slightly higher magnification of the stained cells. Scale bar = 0.25 mm.

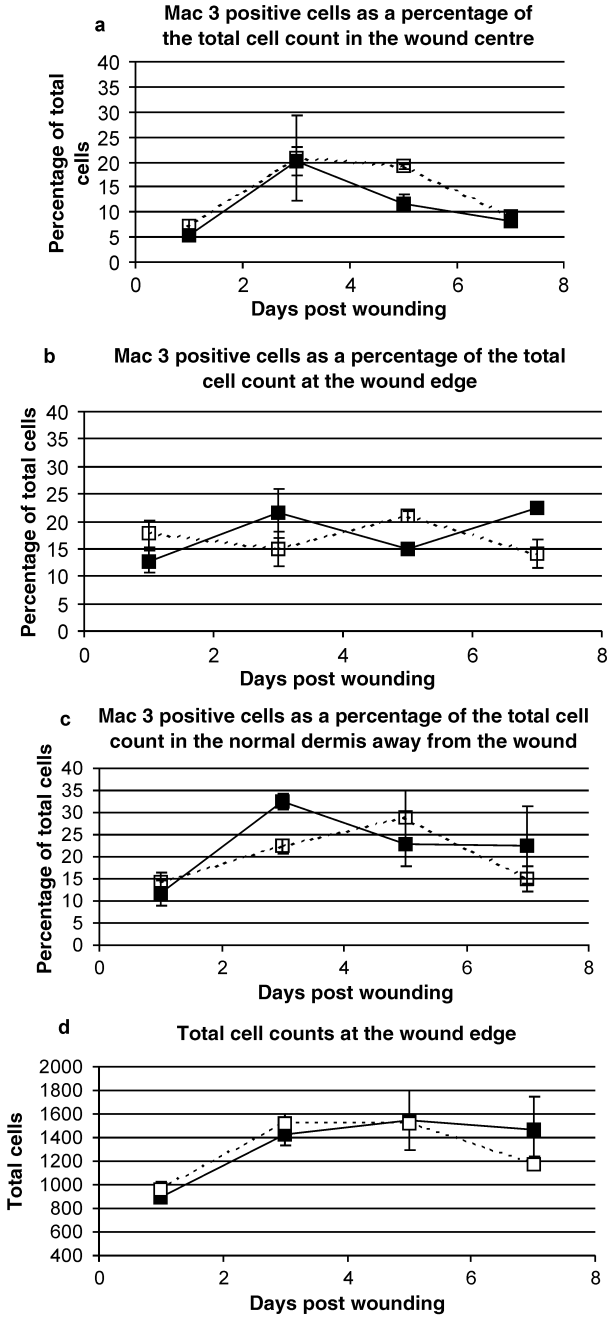

Fig. 8 Mac-3-positive cell counts expressed as a percentage of the total cell count in both MRL/MpJ (closed boxes) and C57BL/6 (open boxes) wounds. Cells were counted at the wound centre (a), wound edge (b) and in the normal dermis away from the wound (c). There was no significant difference in the percentage of Mac-3-positive cells between the two strains in any region at any time point. Total cell counts at the wound edge (d) demonstrate that no significant difference existed between the two strains of mice, suggesting that percentage cell counts are truly representative. Results shown are mean ± SEM, $n = 3$.

muscle actin (α-SMA), a cellular protein vital for wound contraction. The protein was detected in similar quantities in both strains of mouse. The distribution of α-SMA was also consistent, with the majority of protein found in a dense band of myofibroblasts situated between the cut panniculus carnosus and the epidermis (Fig. 9). Cells in the centre of the wound that formed the majority of the granulation tissue did not express the protein at the same intensity. Difficulties in counting myofibroblasts accurately prevented a quantitative assessment of α-SMA expression in these wounds, but there does not appear to be a substantial difference in the expression levels.

The differences between scarring in a back skin wound and regeneration after clinical biopsy ear punch injury are quite striking. An extensive analysis of ear regeneration post-wounding has already been undertaken by ourselves and others (Clark et al. 1998; Rajnoch et al. 2003). However, a useful comparison of the two processes of regeneration and repair can be considered by simply observing how the healing processes differ at the two sites. By day 14, the MRL/MpJ back skin wounds are well granulated and completely re-epithelialized. The granulation tissue was maturing, with increasing collagen deposition and a decrease in cellularity (Fig. 10a). By day 84 post-wounding, MRL/MpJ back skin wounds heal with a scar (Fig. 10b). As noted earlier, hair follicles and sebaceous glands were absent, and the scar matrix was arranged in a parallel, striated pattern as opposed to the basket weave pattern of normal dermis towards the wound edges (Fig. 10a). In the ear punch biopsy wounds, distinct regeneration was observed by day 14 post-wounding (Fig. 10c). Blastema-like structures had formed around the original punch biopsy site, the apical epithelial tip had thickened and downgrowths were observed projecting into the mesenchyme (arrow, Fig. 10c). Mature collagen had also been deposited at the mesenchymal–epithelial junction. By day 84 post-wounding, in the MRL/MpJ ear, the two opposing regenerating blastema-like edges of the wound had fused (Fig. 10d). Mature collagen was laid down and a mesenchymal area containing *de novo* cartilage islands was observed.

Discussion

The MRL/MpJ mouse is capable of regenerating tissue from a through-and-through ear punch wound faster than other mouse strains and without a scar, although

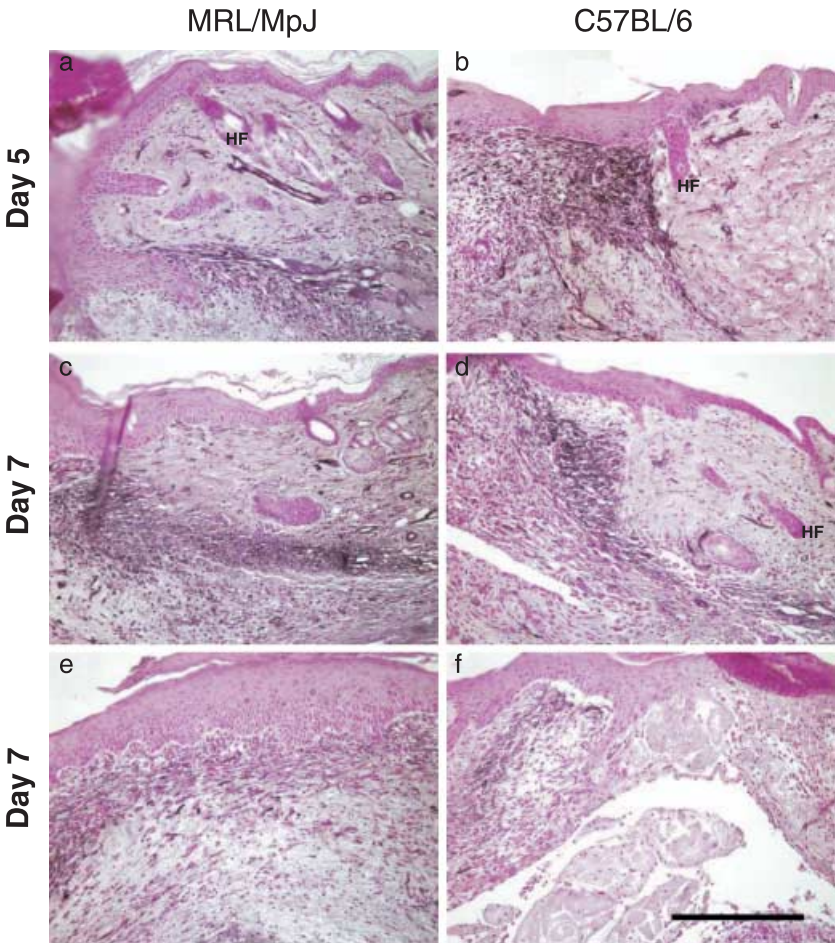

Fig. 9 Alpha smooth muscle actin immunostaining at days 5 (a,b) and 7 (c–f) post-injury in MRL/MpJ (a,c,e) and C57BL/6 (b,d,f) wound sections. Note that the majority of positive staining occurs as a dense band stretching from the cut panniculus to the epidermis at the wound edge, between the dermis and granulation tissue (a–d). By contrast, there is much less staining in the granulation tissue in the centre of the wound (e,f). In this area minimal differentiation of fibroblasts into myofibroblasts has occurred. Also note that the blood vessel smooth muscle cells have stained strongly for α-SMA, as was expected. HF = hair follicle. Scale bar = 0.15 mm.

the mechanism by which it achieves this is not known. By contrast to other reports in the scientific literature, in our studies, C57BL/6 mice heal at least 50% of the original wound area, suggesting that some of the so-called 'poorer healing' strains also have some capacity for regeneration (Rajnoch et al. 2003; Metcalfe & Ferguson, 2005).

Extensive analysis has been carried out in our own laboratory (Rajnoch et al. 2003; Metcalfe & Ferguson, 2005) as well as in others (Clark et al. 1998; McBrearty et al. 1998; Li et al. 2001) on ear regeneration in the MRL/MpJ mouse. The cutaneous portion of the ear punch wound regenerates all the differentiated structures of the ear without scarring (Clark et al. 1998; Rajnoch et al. 2003; Metcalfe & Ferguson, 2005). Until very recently, nothing was known about the healing capabilities of skin wounds created in other locations of the MRL/MpJ body (Colwell et al. 2006). Here, we extended the findings of our earlier study (Rajnoch et al. 2003) describing dorsal excisional skin wounds taken from MRL/MpJ mice with proven regenerative capacity in the ear and compared it with that of the partially regenerative C57BL/6 mice over an extensive time course. We demonstrate that the regenerative capacity observed in the wounded MRL/MpJ mouse ear is not displayed in the healing skin of the wounded backs from the same mice. In fact both strains of mice observed repaired with scarring in response to dermal injury using a 4-mm punch biopsy. Our results also confirm the recent findings of Colwell et al. (2006), who studied wounding in MRL/MpJ back wounds for 28 days post-wounding.

Initially at day 3 post-wounding, the dorsal wound healing observed in this study appeared to show slight differences in the amount of re-epithelialization between the two strains, with the MRL/MpJ wounds demonstrating more epithelial migration than the C57BL/6 wounds at the margins. By day 5 post-wounding, however, this initial enhancement of re-epithelialization was no longer apparent. Between days 5 and 14 dorsal post-wounding, some variation in wound shapes between the two strains were noted.

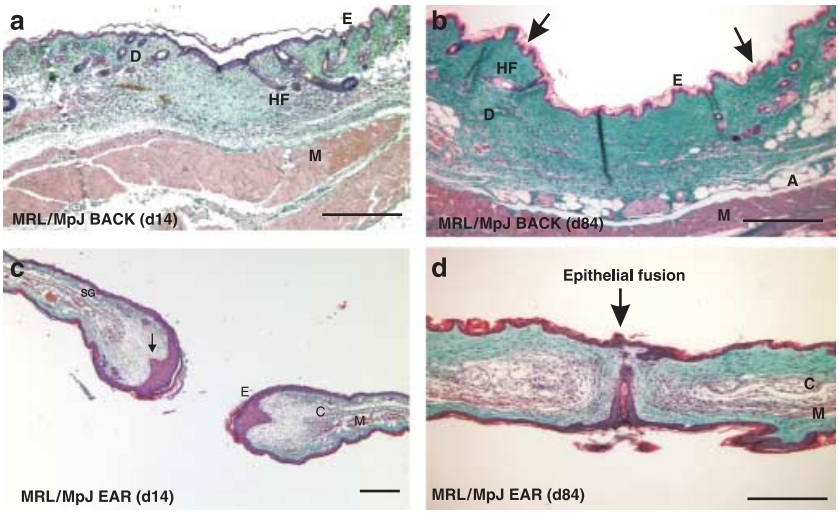

Fig. 10 The histological differences between repair and regeneration in the MRL/MpJ mouse shown at two different time points during healing. Back skin wounds at day 14 post-wounding show full re-epithelialization and maturing granulation tissue (a). By day 84 post-wounding a scar can be seen at the wound centre, devoid of differentiated structures and showing a parallel arrangement of collagen bundles (b). Towards the left- and right-hand wound margins the collagen is more loosely arranged and contains hair follicles (HF), sweat and sebaceous glands as well as adipose tissue (A). (c) A transverse section through an ear, 14 days post-wounding. Two opposing blastema-like structures can be seen with thickened apical epithelial tips and downgrowths projecting into the mesenchymal space (arrowed). The regenerated tissue can be seen from the cut cartilage edge. By day 84 post-wounding in the ear, the two opposing blastema-like structures fuse (d). Cartilage islands are present (C), skeletal muscle is regenerating (M) and the epithelial edges are seen to fuse together (arrow). SG, sebaceous gland; E, epithelium; D, dermis. Scale bar = 0.5 mm.

By day 14, all wounds were well granulated and completely re-epithelialized, the granulation tissue continued to mature, collagen was deposited and a scar began to form. Interestingly no differentiated structures were apparent within the wounded area. This was the first indicator that in both strains the back heals by normal repair and not by regeneration. At day 21 post-wounding the dermis became thinner and the collagen staining matched more closely the surrounding tissue. By the later time points (up to 84 days post-wounding) this poorly differentiated area together with the damaged panniculus carnosus was a good indicator of the wound site as scar integration progressed. Extensive analysis of wound area showed that the MRL/MpJ dorsal wounds did not heal significantly faster than those of the C57BL/6 mice. Inflammation into the wound site was also assessed using a macrophage-specific antibody, Mac-3, and found to be the same for the two strains of mice. Wound contraction was also assessed using α-SMA, and again there was very little difference between the dorsal healing processes in the two strains.

In keeping with the observations of Colwell et al. (2006), this result was surprising as it contrasts quite markedly with earlier results obtained with the same MRL/MpJ mice obtained after 2-mm through-and-through biopsy punching of the ear (Rajnoch et al. 2003). The regeneration of the ear is thought to arise from the development of a regeneration blastema, similar to that seen in regenerating amphibian limbs (Echeverri et al. 2001; Rageh et al. 2002; see reviews by Stocum, 2004; Endo et al. 2004). These blastema-like structures were not observed in our MRL/MpJ dorsal skin wounds but were seen in ear wounds created in the same animals (Rajnoch et al. 2003). Significantly, rather than regenerating like the wounded ears, the dorsal wounds repaired with scarring. This demonstrates that repair and regeneration can occur in the same animal and is dependent upon the location of the injury. This fundamentally important observation suggests that the mechanisms governing these two healing processes are likely to be controlled by similar molecules that subtly diverge along different pathways dependent upon the location of injury (Ferguson & O'Kane, 2004).

The lack of regeneration in the skin of the MRL/MpJ mouse back may be a reflection of differences in the architecture of the two sites. The ear is a very thin structure with epidermis on both sides, as well as containing a supporting cartilage framework. The blastema-like

structures that develop in the wounded ear are manifested adjacent to the cartilage at the wound edge. It may be that the regeneration of the ear is in some way controlled by a number of factors including the deposition of new cartilage, glycosaminoglycans (GAGs) and extracellular matrix (ECM) within the developing primitive mesenchyme of the blastema-like structure (Metcalfe & Ferguson, 2005). It is also probably essential for regeneration that these mesenchyme cells are kept in a de-differentiated state. Molecules like preadipocyte factor-1 (Pref-1), a delta-like protein containing epidermal growth factor-repeats, is expressed in proliferating cells in a variety of tissues and is believed to be involved in this process in the MRL/MpJ ear (Samulewicz et al. 2002). This de-differentiated state may also be brought about in part by a series of signalling cascades set up by the growing tip epithelium of the ear blastema.

By contrast, the skin on the body is loose, much thicker than the ear and with a substantial subcutaneous fat layer. Unlike the ear, there is only one epithelial layer in the back and perhaps equally importantly, no cartilage. Contraction of the back wounds is likely to play an important role in the repair process, while in the ear this is not able to occur to the same extent, with perhaps the result that the alternative mechanism of regeneration is triggered. Mechanotransductive forces on cells are known to play a role in signal transduction pathways, growth factor shedding and cell proliferation (Tschumperlin et al. 2004; Yano et al. 2004; Katsumi et al. 2005). It is thought that cells are able to sense mechanical stress through autocrine loops localized to compliant extracellular spaces (Tschumperlin et al. 2004). If this is the case, then in an injury made on the dorsum such cellular stresses are probably much different from those that impact on cells in the injured ear. This phenomenon is likely to play a significant role in the subsequent mechanisms governing whether a wound closes by simple repair or by scar-less regeneration.

During the response to injury within a tissue, collagen in the skin undergoes dramatic reorganization and matrix metalloproteinases (MMPs) degrade and remodel the collagen in a tightly controlled process. We have previously shown by use of the Collagenase-Resistant mouse that the activity of MMPs on collagen during the earliest stages of wound repair is a critical process. The inability of MMPs to cleave collagen results in severely delayed early healing (Beare et al. 2003). Regenerating amphibian limbs, zebrafish tails, the MRL/MpJ ear, myocardial regeneration in rabbits and fetal skin wounds are all known to have up-regulated MMPs (Dang et al. 2003; Gourevitch et al. 2003; Kato et al. 2003; Hampton et al. 2004; Minatoguchi et al. 2004; Bai et al. 2005). Additionally, MMPs have different effects on regenerative function. During the regenerative process MMPs affect morphogenesis and cell transdifferentiation in hydra (Leontovich et al. 2000), as well as influencing changes in extracellular matrix content during intestine regeneration in the sea cucumber (Quinones et al. 2002). MMPs are also required for normal newt limb regeneration and function, in part to prevent scar formation during the regenerative process (Vinarsky et al. 2005). MMPs may thus preferentially promote regeneration rather than repair by decreasing the amount of collagen being laid down, allowing cells to migrate and penetrate structures more easily.

Vital clues towards the understanding of how regeneration and repair can occur within the same organism may arise from a phenomenon that has long intrigued researchers: differences in limb-forming tissue vs. the flank, which has led to the concept of the limb field. This is the tissue of the embryo that has the potential to form a limb, even when that tissue is grafted or transplanted elsewhere. However, non-limb field embryonic flank tissue can also form a limb if given implants of either limb mesoderm or fibroblast growth factor (FGF)-soaked beads (Cohn et al. 1995; Yonei-Tamura et al. 1999). Nerve-deviation studies also indicate that accessory limbs readily form from upper arm but not flank tissue (Egar, 1988). In addition, flank dermis is inhibitory to limb regeneration (Tank, 1981). The molecular mechanisms behind the regulation of limb outgrowth in limb field as opposed to non-limb field tissues have recently begun to be dissected, the expression of *homeobox* patterning genes correlating well with limb-forming abilities (Cohn et al. 1997; Cohn & Tickle, 1999). FGF pathways are known to be critical to limb outgrowth (Xu et al. 1998; Sekine et al. 1999), and this has led to investigations to clarify whether FGFs might also be involved in the differing limb-forming abilities of flank vs. limb tissues of the Mexican axolotl (Christensen et al. 2002). These same molecules and signalling cascades involved in defining limb field may also play a role in determining how a wound repairs, dependent upon its location, either simply resulting in scar tissue formation or perfectly regenerating in a scar-free way.

In summary, unlike the accelerated regeneration observed in the wounded ears of MRL/MpJ mice, dorsal

wounds created in the same mice heal with scarring, similar to other strains of mice. Macrophage infiltration and smooth muscle actin deposition during dorsal repair were similar in both strains investigated. The most exciting and significant finding of this study is that regeneration and repair can occur simultaneously within the same animal, as has also been noted to occur in humans (Ferguson & O'Kane, 2004). This suggests that similar molecules and signals are likely to be required for both mechanisms but in some way are orchestrated differently, dependent upon the location of injury within the body. These subtle mechanistic differences between repair and regeneration hold great hope for tissue regeneration and engineering because they are experimentally manipulable. Further investigations are ongoing in order to dissect these healing mechanisms further.

Acknowledgements

This work was conducted as part of the UK Centre for Tissue Engineering, generously funded by grants from the BBSRC, MRC and EPSRC (grant no. 34/T1E13617).

References

Ashcroft GS, Horan MA, Ferguson MW (1995) The effects of ageing on cutaneous wound healing in mammals. *J Anat* **187**, 1–26.

Ashcroft GS, Greenwell-Wild T, Horan MA, Wahl SM, Ferguson MW (1999) Topical estrogen accelerates cutaneous wound healing in aged humans associated with an altered inflammatory response. *Am J Pathol* **155**, 1137–1146.

Bai S, Thummel R, Godwin AR, et al. (2005) Matrix metalloproteinase expression and function during fin regeneration in zebrafish: analysis of MT1-MMP, MMP2 and TIMP2. *Matrix Biol* **24**, 247–260.

Beare AH, O'Kane S, Krane SM, Ferguson MW (2003) Severely impaired wound healing in the collagenase-resistant mouse. *J Invest Dermatol* **120**, 153–163.

Christensen RN, Weinstein M, Tassava RA (2002) Expression of fibroblast growth factors 4, 8, and 10 in limbs, flanks, and blastemas of Ambystoma. *Dev Dyn* **223**, 193–203.

Clark LD, Clark RK, Heber-Katz E (1998) A new murine model for mammalian wound repair and regeneration. *Clin Immunol Immunopathol* **88**, 35–45.

Cohn MJ, Izpisua-Belmonte JC, Abud H, Heath JK, Tickle C (1995) Fibroblast growth factors induce additional limb development from the flank of chick embryos. *Cell* **80**, 739–746.

Cohn MJ, Patel K, Krumlauf R, Wilkinson DG, Clarke JD, Tickle C (1997) Hox9 genes and vertebrate limb specification. *Nature* **387**, 97–101.

Cohn MJ, Tickle C (1999) Developmental basis of limblessness and axial patterning in snakes. *Nature* **399**, 474–479.

Colwell AS, Krummel TM, Kong W, Longaker MT, Lorenz P (2006) Skin wounds in the MRL/MPJ mouse heal with scar. *Wound Repair Regen* **14**, 81–90.

Dang CM, Beanes SR, Lee H, Zhang X, Soo C, Ting K (2003) Scarless fetal wounds are associated with an increased matrix metalloproteinase-to-tissue-derived inhibitor of metalloproteinase ratio. *Plast Reconstr Surg* **111**, 2273–2285.

Echeverri K, Clarke JD, Tanaka EM (2001) In vivo imaging indicates muscle fiber dedifferentiation is a major contributor to the regenerating tail blastema. *Dev Biol* **236**, 151–164.

Egar MW (1988) Accessory limb production by nerve-induced cell proliferation. *Anat Rec* **221**, 550–564.

Endo T, Bryant SV, Gardiner DM (2004) A stepwise model system for limb regeneration. *Dev Biol* **270**, 135–145.

Ferguson MW, O'Kane S (2004) Scar-free healing: from embryonic mechanisms to adult therapeutic intervention. *Philos Trans R Soc Lond B Biol Sci* **359**, 839–850.

Gawronska-Kozak B (2004) Regeneration in the ears of immunodeficient mice: identification and lineage analysis of mesenchymal stem cells. *Tissue Eng* **10**, 1251–1265.

Gawronska-Kozak B, Bogacki M, Rim JS, Monroe WT, Manuel JA (2006) Scarless skin repair in immunodeficient mice. *Wound Repair Regen* **14**, 265–276.

Goss RJ, Grimes LN (1975) Epidermal downgrowths in regenerating rabbit ear holes. *J Morph* **146**, 533–542.

Gourevitch D, Clark L, Chen P, Seitz A, Samulewicz SJ, Heber-Katz E (2003) Matrix metalloproteinase activity correlates with blastema formation in the regenerating MRL mouse ear hole model. *Dev Dyn* **226**, 377–387.

Hampton DW, Seitz A, Chen P, Heber-Katz E, Fawcett JW (2004) Altered CNS response to injury in the MRL/MpJ mouse. *Neuroscience* **127**, 821–832.

Kato T, Miyazaki K, Shimizu-Nishikawa K, et al. (2003) Unique expression patterns of matrix metalloproteinases in regenerating newt limbs. *Dev Dyn* **226**, 366–376.

Katsumi A, Naoe T, Matsushita T, Kaibuchi K, Schwartz MA (2005) Integrin activation and matrix binding mediate cellular responses to mechanical stretch. *J Biol Chem* **280**, 16546–16549.

Leontovich AA, Zhang J, Shimokawa K, Nagase H, Sarras MP (2000) A novel hydra matrix metalloproteinase (HMMP) functions in extracellular matrix degradation, morphogenesis and the maintenance of differentiated cells in the foot process. *Development* **127**, 907–920.

Li F, Jin F, Freitas A, Szabo P, Weksler ME (2001) Impaired regeneration of the peripheral B cell repertoire from bone marrow following lymphopenia in old mice. *Eur J Immunol* **31**, 500–505.

Li X, Mohan S, Gu W, Miyakoshi N, Baylink DJ (2000) Differential protein profile in the ear-punched tissue of regeneration and non-regeneration strains of mice: a novel approach to explore the candidate genes for soft-tissue regeneration. *Biochim Biophys Acta* **1524**, 102–109.

Li X, Mohan S, Gu W, Baylink DJ (2001) Analysis of gene expression in the wound repair/regeneration process. *Mamm Genome* **12**, 52–59.

Masinde GL, Li X, Gu W, Davidson H, Mohan S, Baylink DJ (2001) Identification of wound healing/regeneration quantitative trait loci (QTL) at multiple time points that explain

seventy percent of variance in (MRL/MpJ and SJL/J) mice F2 population. *Genome Res* **11**, 2027–2033.

Masinde GL, Li X, Baylink DJ, Nguyen B, Mohan S (2005) Isolation of wound healing/regeneration genes using restrictive fragment differential display-PCR in MRL/MPJ and C57BL/6 mice. *Biochem Biophys Res Commun* **330**, 117–122.

McBrearty BA, Clark LD, Zhang XM, Blankenhorn EP, Heber-Katz E (1998) Genetic analysis of a mammalian wound-healing trait. *Proc Natl Acad Sci USA* **95**, 11792–11797.

Metcalfe AD, Ferguson MW (2005) Harnessing wound healing and regeneration for tissue engineering. *Biochem Soc Trans* **33**, 413–417.

Minatoguchi S, Takemura G, Chen XH, et al. (2004) Acceleration of the healing process and myocardial regeneration may be important as a mechanism of improvement of cardiac function and remodeling by postinfarction granulocyte colony-stimulating factor treatment. *Circulation* **109**, 2572–2580.

Quinones JL, Rosa R, Ruiz DL, Garcia-Arraras JE (2002) Extracellular matrix remodelling and metalloproteinase involvement during intestine regeneration in the sea cucmber *Holothuria glaberrima*. *Dev Biol* **250**, 181–197.

Rageh MA, Mendenhall L, Moussad EE, Abbey SE, Mescher AL, Tassava RA (2002) Vasculature in pre-blastema and nerve-dependent blastema stages of regenerating forelimbs of the adult newt, Notophthalmus viridescens. *J Exp Zool* **292**, 255–266.

Rajnoch C, Ferguson S, Metcalfe AD, Herrick SE, Willis HS, Ferguson MW (2003) Regeneration of the ear after wounding in different mouse strains is dependent on the severity of wound trauma. *Dev Dyn* **226**, 388–397.

Samulewicz SJ, Seitz A, Clark L, Heber-Katz E (2002) Expression of preadipocyte factor-1 (Pref-1), a delta-like protein, in healing mouse ears. *Wound Repair Regen* **10**, 215–221.

Sekine K, Ohuchi H, Fujiwara M, et al. (1999) Fgf10 is essential for limb and lung formation. *Nat Genet* **21**, 138–141.

Stocum DL (2004) Amphibian regeneration and stem cells. *Curr Top Microbiol Immunol* **280**, 1–70.

Tank PW (1981) The ability of localized implants of whole or minced dermis to disrupt pattern formation in the regenerating forelimb of the axolotl. *Am J Anat* **162**, 315–326.

Tschumperlin DJ, Dai G, Maly IV, et al. (2004) Mechanotransduction through growth-factor shedding into the extracellular space. *Nature* **429**, 83–86.

Ueno M, Lyons BL, Burzenski LM, et al. (2005) Accelerated wound healing of alkali-burned corneas in MRL mice is associated with a reduced inflammatory signature. *Invest Ophthalmol Vis Sci* **46**, 4097–4106.

Vinarsky V, Atkinson DL, Stevenson TJ, Keating MT, Odelberg SJ (2005) Normal newt limb regeneration requires matrix metalloproteinase function. *Dev Biol* **279**, 86–98.

Whitby DJ, Ferguson MW (1991a) Immunohistochemical localization of growth factors in fetal wound healing. *Dev Biol* **147**, 207–215.

Whitby DJ, Ferguson MW (1991b) The extracellular matrix of lip wounds in fetal, neonatal and adult mice. *Development* **112**, 651–668.

Xu X, Weinstein M, Li C, et al. (1998) Fibroblast growth factor receptor 2 (FGFR2) -mediated reciprocal regulation loop between FGF8 and FGF10 is essential for limb induction. *Development* **125**, 753–765.

Yannas IV (2001) *Tissue and Organ Regeneration in Adults*. New York: Springer.

Yano S, Komine M, Fujimoto M, Okochi H, Tamaki K (2004) Mechanical stretching in vitro regulates signal transduction pathways and cellular proliferation in human epidermal keratinocytes. *J Invest Dermatol* **122**, 783–790.

Yonei-Tamura S, Endo T, Yajima H, Ohuchi H, Ide H, Tamura K (1999) FGF7 and FGF10 directly induce the apical ectodermal ridge in chick embryos. *Dev Biol* **211**, 133–143.

Yu H, Mohan S, Masinde GL, Baylink DJ (2005) Mapping the dominant wound healing and soft tissue regeneration QTL in MRL × CAST. *Mamm Genome* **16**, 918–924.